WARSAW UNIVERSITY OF TECHNOLOGY Index 351733
FACULTY OF CIVIL ENGINEERING
COMMITTEE FOR CIVIL AND WATER ENGINEERING
POLISH ACADEMY OF SCIENCES ISSN 1230-2945
DOI: 10.24425/ace.2024.148916
ARCHIVES OF CIVIL ENGINEERING
Vol. LXX ISSUE 1 2024
pp. 357 –373

Research paper

Evaluation of using hardening soil model for predicting wall deflections caused by deep excavation: A case study at the Ho Chi Minh metro line 1, Vietnam

Luc Manh Bui[1], Li Wu[2], Yao Cheng[3], Dao Jun Dong[4]

Abstract: The goal of this study is to assess the application of the Hardening soil model in predicting the deformation of retaining walls of excavations in 2D and 3D finite element analysis at the Ho Chi Minh Metro project. Designed as the deepest underground station in the first metro line built in Ho Chi Minh City (HCMC), Opera House station is located in an area with a dense building zone and close to historical buildings. A summary of the input soil properties is provided using data from site investigations, in-situ tests, and laboratory tests. By numerical simulation using the Hardening soil model, the parameters of the soil stiffness modulus value are verified based on the Standard Penetration Test (SPT), and Pressuremeter test (PMT). The obtained results of the numerical analysis by 2D and 3D finite element methods, and field observations indicate that applying the Hardening soil model with soil stiffness modulus obtained in situ tests gives reasonable results on the displacement of the retaining wall at the final phase. The relationship between the SPT value and the stiffness modulus of HCMC sand is a function of depth. This correlation is obtained through the comparison of wall deformation between the simulation and monitoring at the construction site. The results of the difference between 2D and 3D finite element analysis also are discussed in this study.

Keywords: deep excavation, Ho Chi Minh MRT, hardening soil model, opera house station, wall deflections

[1]PhD student, Eng., Faculty of Engineering, China University of Geosciences (Wuhan), No. 388 Lumo Road, Wuhan 430074, Hubei, China, e-mail: lucbui.uctgeo@gmail.com, ORCID: 0009-0006-7816-8796
[2]Prof., PhD., Eng., Doctoral supervisor, Faculty of Engineering, China University of Geosciences (Wuhan), No. 388 Lumo Road, Wuhan 430074, Hubei, China, e-mail: lwu@cug.edu.cn, ORCID: 0000-0001-9651-3772
[3]Assoc. Prof., PhD., Eng., Doctoral supervisor, Faculty of Engineering, China University of Geosciences (Wuhan), No. 388 Lumo Road, Wuhan 430074, Hubei, China, e-mail: chengyao@cug.edu.cn, ORCID: 0000-0003-2925-2773
[4]Assoc. Prof., PhD., Eng., Doctoral supervisor, Faculty of Engineering, China University of Geosciences (Wuhan), No. 388 Lumo Road, Wuhan 430074, Hubei, China, e-mail: 66826130@qq.com, ORCID: 0009-0005-9055-5564

1. Introduction

As the largest city in the south of Vietnam, the increase in population and traffic volume in recent years has put great pressure on the transport infrastructure of Ho Chi Minh City. With the surface land fund for transport infrastructure almost fully exploited, the construction of underground traffic works in urban areas is one of the inevitable solutions. To solve traffic jams and improve the quality of the air environment for city residents, plans have been put forward by the city government, in which it is expected that 8 Metro lines will be built. Ho Chi Minh Line 1 (Ben Thanh-Suoi Tien) is the first line built with a total length of 19.7 km, including 2.5 km underground and 17.6 km on the viaduct. In addition to using the Tunneling Boring Method (TBM) (first used in Vietnam), minimizing the impact from the construction of underground stations with a great depth in an area with high construction density and next to other underground stations. Historical works are always a challenge for design engineers.

The fact that the high sand content was found through field investigations at the Opera House station has caused certain difficulties in determining the input parameters of the model. As a common problem during deep sand excavation is that the test data are limited and of low quality due to the difficulty of obtaining an intact sample. Therefore, the strength parameters of the sand can be obtained directly from the experiments, but the stiffness parameters are very difficult to obtain precisely. In the studies on the deformation of retaining walls caused by the construction of excavation pits. It can be seen that the parameters of soil hardness have the most significant influence on the deformation of retaining walls.

Nikolinakou et al. [1] conducted an analysis of the case of a dug hole in the sand in Berlin that involved an extensive program of laboratory experiments and the application of a relatively elastic soil model. Although the results show good agreement between observations and calculations, this study also demonstrates the complexity involved in measuring important soil properties and the selection of model parameters. Ou et al. [2] used the hyperbolic model in the analysis and the SPT-N values through the shear wave velocity equations to determine Young's modulus of the sand and mud in Taipei, Taiwan. Module Young of sand and mud in Taipei, Taiwan was determined by Ou et al. [2] using a hyperbolic model based on SPT-N values obtained through shear wave velocity equations. A linear-elastic perfect plastic model was applied by Hsiung [3] for numerical simulations of deep excavations in the sand at Kaohsiung. This approach established a direct correlation between E and the employed SPT value. In addition, the prediction of deep excavation displacement and the influence of the 3D excavation simulation on the deflection of the wall was assessed by Hsiung [4] using the HS model based on the relationship between E and SPT-N values. These studies collectively underscore the practicality of field soil testing data in selecting calculation parameters for deep-excavations deformation analysis. However, the investigations conducted by both Ou et al. and Hsiung [2–4] reveal that the soil hardness parameter, deduced from the outcomes of the SPT experiment, exhibits significant variability across diverse sands within distinct study sites. In this study, a 3-D simulation model with full structural components was established, and the retaining wall deflection results were compared with the basic 2D model results. From here, a new plane strain ratio (PSR) ratio was established and compared with previous studies performed for sand by Ou and Hsiung [2, 4]. Along with that, the selected hard soil model for this analysis is

based on empirical formulas of the relationship between the stiffness modulus and the SPT-N value, the field lateral compression test PMT and the stiffness correlation of soil and SPT-N values proposed in this study for sand and clay layers at Opera House station as a case study in Vietnam. In this study, the soil stiffness modulus from different methods was used for modeling the displacement of the retaining wall, and a new equation for computing soil stiffness modulus was proposed. Then, the retaining wall deformation of excavation was calculated from different predicted methods and measured values were compared and discussed. In addition, a function of soil hardness modulus with depth is provided based on good agreement from predictions and field observations.

2. Project information and background

2.1. Conditions of the excavation site

In this study, a deep excavation in Ho Chi Minh City Mass Rapid (HCMC-MRT) line 1 was chosen as a case study. Opera House Station is an underground station located at the junction of Le Loi Street and Nguyen Hue Street (Fig. 1). The excavation length is 228 m with the width changes from 23 m to 47.45 m for different sections. The top-down method was used, including 10 excavation phases. The excavation stages were supported by 5 levels of reinforced concrete slabs with different thicknesses.

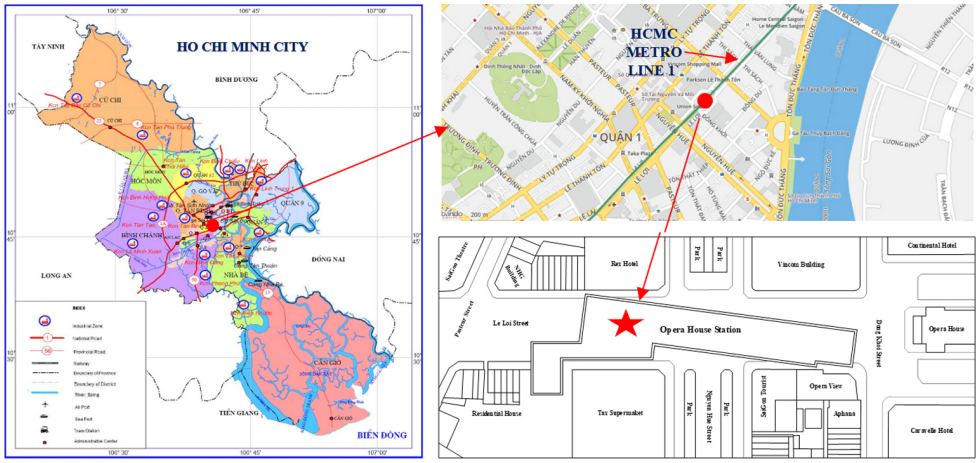

Fig. 1. The location of the excavation site

In the final excavation stage, the maximum depth of excavation was 33.2 m. A diaphragm wall with a thickness of 1.5 m and 44 m depth was used to retain the excavated pit. The cross-section of the excavation is shown in Fig. 2. The H-458 × 417 × 30 × 50 steel beams were set up as kingposts in the mid of the excavation area and strut system to enhance the stiffness of the retaining wall. The H-beam was inserted 4.5 m into bored piles with a diameter of 1.5 m.

In addition, a strut system H-458 × 417 × 30 × 50 is inclined, connecting the wall system and the main beams (Fig. 3), the distance between struts is approximately 2.5 m. Details of the detailed installation sequence of the strut system are shown in Table 1.

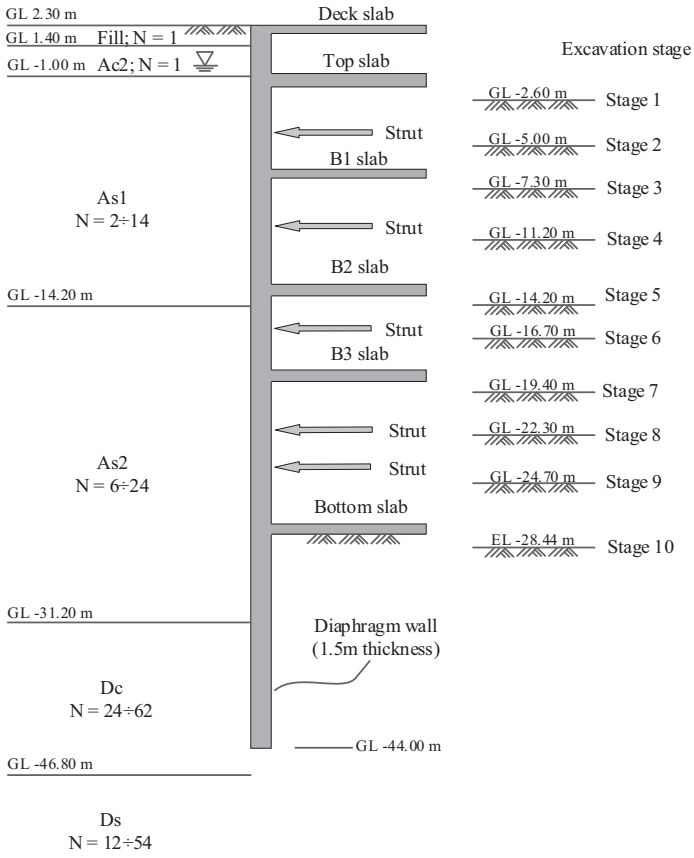

Fig. 2. The profile of subsurface soils and the excavation process

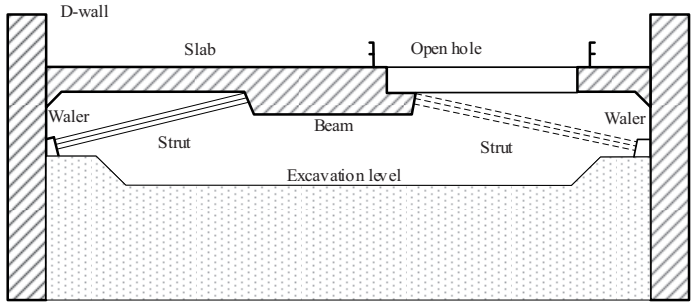

Fig. 3. Cross section of the excavation and strutting system

Table 1. Construction steps of the excavation

Phases	Construction sequences
1	Diaphragm wall installation and King post
2	Excavation for Temporary RC slab deck (slab thickness, t = 0.5 m)
3	Construction of Temporary RC slab deck
4	Excavation for roof Slab level (slab thickness, t = 0.8 m)
5	Construction of roof slab
6	Excavation for strut 1 – Waling
7	Construction of Waling & Strut 1
8	Excavation for B1F level (slab thickness, t = 0.5 m)
9	Construction of B1F
10	Excavation for strut 2 – Waling & Removal of Strut 1
11	Construction of Waling & Strut 2
12	Excavation for B2F level (slab thickness, t = 0.6 m)
13	Construction of B2F
14	Excavation for strut 3 – Waling & Removal of Strut 2
15	Construction of Waling & Strut 3
16	Excavation for B3F level (slab thickness, t = 0.6 m)
17	Construction of B3F
18	Excavation for strut 4 – Waling & Removal of Strut 3
19	Construction of Waling & Strut 4
20	Excavation for strut 5 – Waling & Removal of Strut4
21	Construction of Waling & Strut 5
22	Excavation for Base slab level
23	Base slab casting (slab thickness, t = 0.3 m)

As shown in Fig. 2, the excavation box is completely embedded in a thick sand layer with highly permeable, classified into two main layers namely: As1 and As2. Depth from the ground surface is approximately 3 m, layer As1 consists mainly of reddish brown to yellowish-brown, very loose to medium dense, silty clayey sand, with thickness varying from 10 m to 23 m, the SPT-N value from this layer range from 2 to 14. Layer As2 consists mainly of reddish brown to yellowish brown, loose to medium dense, fine to medium grain sand, and was encountered immediately below As1 with a thickness of 16.8 m to 17.2 m, the SPT-N value of As2 layer range 6 to 24. The diaphragm wall toe is in the Dc layer (30.5 to 32.3 below the surface), which has low permeability, thus reducing the water penetrating into the base of the excavation. Dc layer consists mainly of brown to light grey, medium stiff to hard clay, encountered underneath layer As2 with thickness varying from 15 m to 15.9 m, the SPT-N value of this layer range from 24 to 62.

Fill is composed predominantly of brown to dark brown mixtures of clay, sand, gravel, construction debris, and organic material. It covers the entire site area with a thickness from 0.5 to 1.2 m, the SPT-N value of the fill layer is absent. Ac2 layer was encountered immediately below the fill layer, with thickness varying from 1 to 1.8 m, Ac2 consists mainly of brownish grey to grey, very soft to stiff clay with traces of organic material, and the SPT-N value of this layer range from 1 to 2. Due to the survey depth of the boreholes stopping at 65 m under the ground surface, the Ds layer depth is not fully investigated. The Ds layer consists mainly of light grey, dense to very dense silty sand, this layer was encountered at depths of 46.4 m to 50.5 m, and the SPT-N value of this Ds ranges from 12 to 54.

2.2. In-situ monitoring and observation

Different monitoring instruments such as inclinometer, kingpost strain gauges, observation well, and surface settlement points were set up around and nearby the excavation site to monitor and. All monitoring data were collected, then the data was carefully checked to take reliable data for analysis and discussion (Fig. 4).

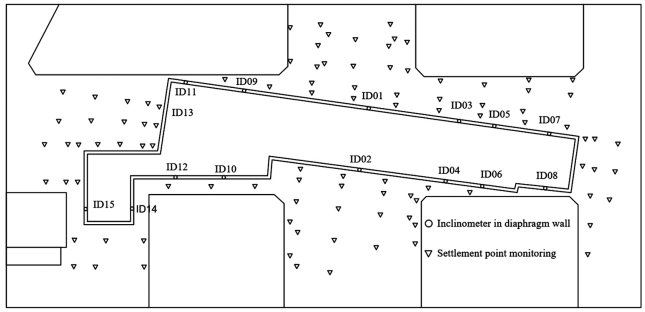

Fig. 4. Position of the observation instrument

The inclinometer shown in Fig. 4, in which the data from eight monitoring points (ID01 to ID08) was used for modeling. First, the lateral deformation of the retaining wall was observed and examined. Indeed, the wall first behaved in cantilever mode, and then when the struts were ensembled, the behavior of the wall changes to prop mode.

2.3. Soils test and determination of soil properties

2.3.1. In-situ soil tests

Figure 5 presents detailed information from eight boreholes located nearby the excavation site, including the profiles of the Atterberg limits (PL, W, and LL), and void ratio.

It can be seen that the plastic limit (PL) ranges from 10 to 40% and is mostly located around 20%. Similarly, the water content (W) is mainly concentrated around 20%. The limit liquid (LL) had a wide range of 10 to 60% and LL is also mostly located at around 20%. At a depth of 5 m, the value ranges from 20 to 60%. The void ratio (e) is in the range of 0.5 to 2.5,

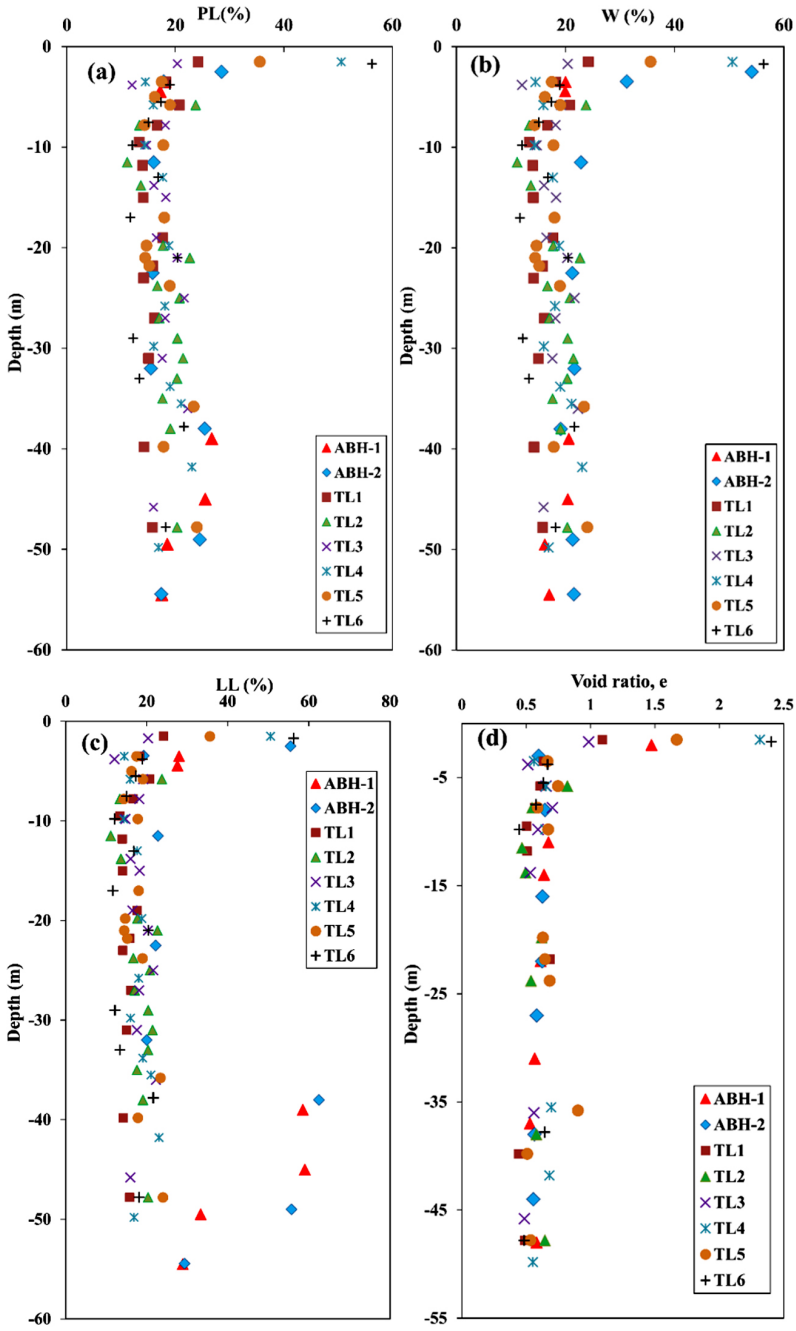

Fig. 5. Information from drilling hole: (a) PL, (b) moisture content (w), (c) LL, and (e) void ratio

and the values of PL, W, and LL range from 20 to 40%. The sand content has a range of 60 to 100%, while the silt content is in a range of 0 to 10%. The clay content reduces with depth and is mostly smaller than 10%, and some points are greater than 20%. The void ratio is in a range from 0.5 to 0.7.

It is accepted that the SPT test is a popular and simple test, the result of the SPT test is widely used and applied for many aspects of designing foundations. Figure 6 shows the change of SPT-N values with depth. It can be seen that the SPT-N values generally increase with depth. The SPT-N values are greater than 20 when the depth is greater than 35 m. Besides, a series of PMT was conducted to determine deformation parameters that were used for modeling in this study. The maximum depths of the boreholes for E-PMT were around 45 m as shown in Fig. 6.

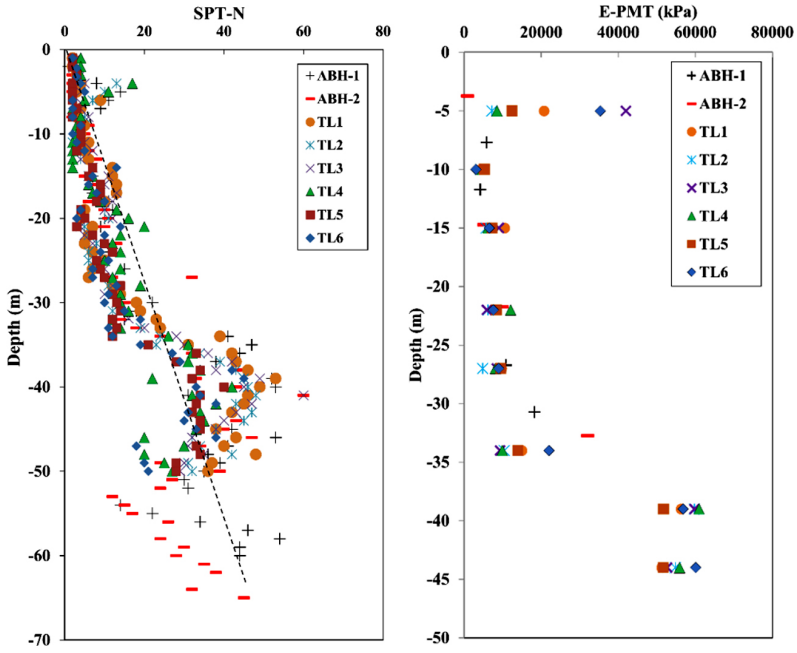

Fig. 6. The result of SPT-N and E-PMT

The results of SPT-N and PMT-Ep are shown in Figure 6. It can be seen that the values of SPT-N generally increase with increasing depth. From 0 to 30 m depth, the values of SPT-N are smaller than 20. When the depth is greater than 30 m, the SPT-N values are in the range of 20 to 50. The values of PMT-Ep are smaller than 20000 kPa when the depth is smaller than 35m. The PMT-Ep values are approximately 60000 kPa when the depth is from 40 to 45 m.

2.3.2. Properties of soil modulus

Indeed, different soil models have been employed for excavation modeling in many previous studies. For example, three constitutive models for soil, including Mohr-Coulomb (MC), Schofield model, and BRICk model have been employed to simulate the wall deformation

caused by deep excavation in London clay Powire et al. [5]. They indicated that the wall deformation predicted by the finite element (FE) analyses is dependent more on the soil stiffness modulus than on the soil model. Nevertheless, the calculation of ground displacement are strongly dependent on both the soil model and soil stiffness modulus. The interaction between soil and structure for excavation in London clay was precisely analyzed using a non-linear soil model Jardine et al. [6]. Furthermore, the excavation of the Queen Elizabeth II Conference Centre in London Clay was investigated and analyzed using two soil moduli, including undrained and drained. For clay layer, Duncan and Buchignani [16] suggested that E was linearly proportional to undrained shear strength S_u, with OCR = 1; $30 < PI < 50$, the ratio E_u/S_u set 300 to 600. The soil modulus can be determined directly from the laboratory via triaxial compression or oedometer tests and from field tests such as PMT, or soil modulus can be computed from the results of SPT or CPT. The relationship between E and N for different soil was proposed by Stroud [7], and he indicated that the increase of soil strain leads to a decrease of E. Hsiung [8] and Yong [9] proposed that E can be calculated using the following equation when the strain range of a retaining wall is approximately 0.1%.

(2.1a) $$E = 4000 \cdot N \quad \text{for clay}$$

(2.1b) $$E = 2000 \cdot N \quad \text{for sand}$$

Besides, the soil modulus E can be estimated using $E = 2800 \cdot N$, which was proposed by the Architectural Institute of Japan [10]. Furthermore, it was reported that the soil modulus obtained from the PMT test was close to the initial modulus (E_i). According to Hsiung [8] the soil modulus from the PMT test shown in Fig. 6 can be set E_{50}^{ref} for modeling.

3. Finite element analysis and modeling

3.1. Soil model and input properties

The excavation in this study is simulated using finite element (FE) analysis. For the FE analysis, the PLAXIS 2D and 3D software were used for modeling. Figure 7 shows 3D FE model for excavation. The FE model consists of 229,651 ten-node tetrahedral elements with a total of 359,513 nodes. The dimensions of the FE model are $210 \times 185 \times 90$ m. The bottom of the model was located in the DS layer, which is 90 m depth from the ground surface. The distance from the retaining wall to the lateral boundaries was set to be 105 m, which is estimated about seven times of excavation depth, this was proposed by Khoiri and Ou [11]. For the whole FE model, the standard fixed condition was used. Horizontal and vertical movements were restrained on lateral and bottom boundaries. The detail of the model and structural elements are shown in Fig. 7.

This study investigates the 2D and 3D influence of the excavation on the displacement of the retaining wall. It was reported that the constitutive soil model used for numerical analysis had a minor effect on the calculated wall deformation [2, 5, 12–14]. Furthermore, in some cases, the soil properties are not enough, and an advanced constitutive soil model in Plaxis analysis takes a computational cost. This study is aimed to use a simple and rational HS soil

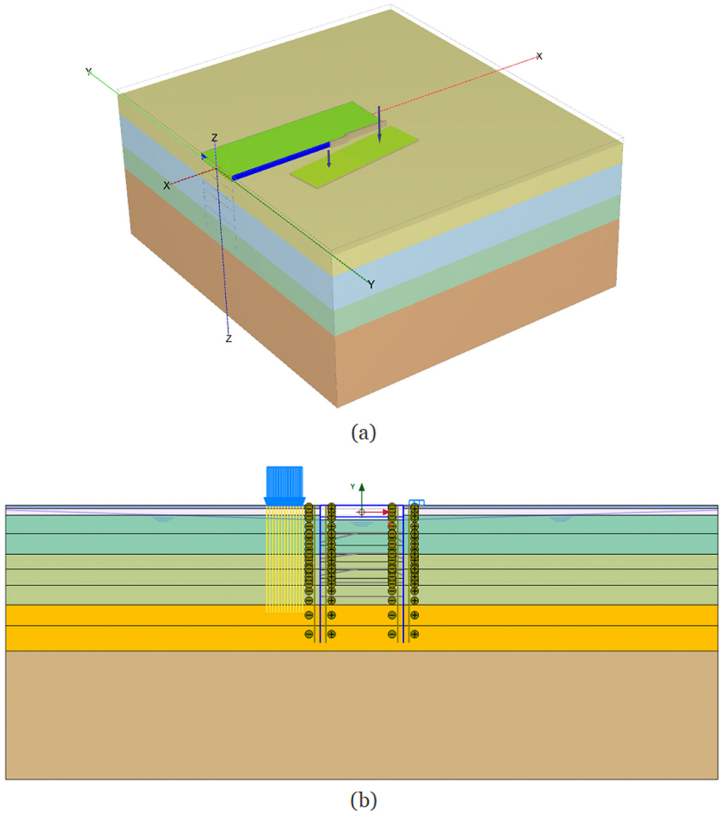

Fig. 7. FE model of the excavation: (a) 3D benchmark model; (b) 2D benchmark model

model using parameters, which can be easily achieved from laboratory or field tests to estimate wall displacement of an excavation.

The input parameters used in modeling for sand and clay layers in modeling are shown in Tables 2 and 3. For the sand layer, an effective stress analysis was conducted, while the total stress analysis was applied for the clay layer under undrained conditions. To avoid instability and problems that happened in PLAXIS calculation, the cohesion value of sand was set to be $c_0 = 0.5$ kPa. The drained Poisson's ratio for sand was set to be $\nu_0 = 0$ as proposed in the previous study [8] and PLAXIS 3D. For the case of sand with friction angle $\varphi > 30°$, the dilation angle is computed as follows:

$$\Psi = \phi' - 30° \tag{3.1}$$

For the clay layers, the undrained friction angle $\varphi_u = 0°$, undrained Poisson's ratio $\nu_u = 0.5$, and undrained dilation angle $\psi_u = 0°$ were used in the MC model. The values of S_u were obtained from the triaxial compression test for the unconsolidated-undrained case. The modulus of sand and clay layers using different methods were calculated and taken from the field and laboratory tests and shown in Table 3.

Table 2. Input parameters of the HS model for sand and clay layers

Layer	NSPT	γ_{sat} (kN/m^3)	γ_{unsat} (kN/m^3)	φ' (°)	c' (kN/m^2)	S_u	ψ'	ν'_{ur}	ν	Coefficient of permeability K (m/day)	Material type
Fill	–	19	18	23	3.7	–	0	0.2	1	1.00E-06	Drained
Ac2	1	16.5	16	–	–	12	0	0.2	1	1.00E-09	Undrained B
As1	6	20	19.5	40	0.5	–	10	0.2	0.5	2.00E-05	Drained
As2	9	20	19.5	40.1	0.5	–	10.1	0.2	0.5	1.00E-05	Drained
Dc	40	21	20.5	–	–	240	0	0.2	1	1.00E-08	Undrained B
Ds	35	21	20.5	34	0.5	–	4	0.2	0.5	1.00E-05	Drained

Table 3. The modulus of soil using different approaches

Layer	Soil Modulus: 2000N and 4000N (Hsiung) [8]			Soil Modulus: 2800N (JP) [10]			Soil Modulus: PMT test		
Soil layer	E_{50}^{ref}	E_{oed}^{ref}	E_{ur}^{ref}	E_{50}^{ref}	E_{oed}^{ref}	E_{ur}^{ref}	E_{50}^{ref}	E_{oed}^{ref}	E_{ur}^{ref}
Fill	2125	2125	6375	2125	2125	6375	2125	2125	6375
Ac2	3468	3468	10404	2436	2436	7308	4200	4200	12600
As1	10440	10440	31320	16800	16800	50400	10530	10530	31600
As2	24360	24360	73080	39200	39200	117600	22030	22030	66090
Dc	149124	149124	447372	104748	104748	314244	61000	61000	183000
Ds	62000	62000	186000	86800	86800	260400	77500	77500	232500

Note: $E_{oed}^{ref} = E_{50}^{ref}$ and $E_{ur}^{ref} = 3E_{50}^{ref}$; E_{ur}^{ref} is the reference moduli for unloading/reloading and E_{oed}^{ref} is the reference moduli for oedometer loading.

3.2. Structural model and input properties

Tables 4–8 show the input parameters of the diaphragm wall, slab parameters, strut parameters, beam parameters, and waling parameters used in the model. The plate element was applied for the diaphragm wall, while the node-to-node anchor element was used for the struts. The input parameters for both plate and node-to-node elements are Young's modulus and Poisson's ratio. The Poisson's ratio for both strut and diaphragm wall was 0.2. The formula of ACI committee 318 was used to compute the Young's modulus of the diaphragm wall [15], the formula is as follows:

$$E = 4700\sqrt{f'_c} \tag{3.2}$$

where f_c' denotes the concrete compressive strength of the concrete. In this study, Young's modulus of the strut was 2.1×10^5 (MPa). To consider cracks and defects of the diaphragm wall and account forstiffness reduction of the strut due to improper installation, the stiffness of the wall and struts were reduced by 30% and 40% in comparison with nominal values, respectively Hsiung [4]. To characterize the interaction between soil and the wall, the interface element was also employed for simulation. The interface reduction parameter between soil and wall is assumed as Rinter = 0.67 based on the suggestion by Khoiri and Ou [11] and the default value suggested by PLAXIS 3D.

Table 4. Diaphram wall parameters

Parameter	Name	Value	Unit
Thickness	d	1.5	m
Young's modulus	E	24870062	kPa
70% Young's modulus	70%E	17409044	kPa
Poission's ratio	v	0.2	

Table 5. Slab parameters

Slabs	d (m)	v	E	80%E (MPa)
Deck slab	0.5	0.15	23025204	18420163
Top slab	0.8	0.15	23025204	18420163
B1-slab	0.5	0.15	23025204	18420163
B2-slab	0.6	0.15	23025204	18420163
B3-slab	0.6	0.15	23025204	18420163
Bottom slab	0.3	0.15	23025204	18420163

Table 6. Strut parameters

Strut No	Types	Section area (m^2)	γ (kN/m^3)	E (kN/m^2)	70%E (kN/m^2)	$I2$ (m^4)	$I3$ (m^4)
Strut 1; 2; 3; 4	H – 458 × 417 × 30 × 50	0.0528	78.5	2.10E+08	1.47E+08	1.87E-03	6.05E-04

Table 7. Beam parameters

Beam No	Section area (m^2)	γ (kN/m^3)	E (kN/m^2)	I2 (m^4)	I3 (m^4)
1	1.62	25	2.30E+07	1.09E-01	4.37E-01
2	1.62	25	2.30E+07	1.09E-01	4.37E-01

Table 8. Waling parameters

Waling No	Types	Section area (m^2)	γ (kN/m^3)	E (kN/m^2)	I2 (m^4)	I3 (m^4)	v
1	H – 400	0.021	78.5	2.10E+08	2.20E-04	2.20E-04	0.15

4. Result and discussion

4.1. Comparison between measured and predicted results for 2D models

The comparison of the measured and predicted wall deformation from different methods at the excavation phase for eight monitoring points is shown in Fig. 8. The result of wall deformation in this study is simulated using the soil modulus $E_{50} = 2500N$ with As1, As2 layers; $E_{50} = 300S_u$ with Ac2 layer; $E_{50}500S_u$ with DC layer. In general, it can be seen that the wall deformation obtained from the measured results is smaller than the predicted values from different methods for eight monitoring points. Besides, the comparison indicated that the application of $E_{50} = 2800N$ is in good agreement with the measured wall deformation results. These results are different from the results found in the previous study conducted by Hsiung [8]. In addition, from the figure, it can be seen that the result of the proposed soil modulus $E_{50} = 2500N$ with As1, As2 layers; $E_{50} = 300S_u$ with Ac2 layer; $E_{50} = 500S_u$ with DC layer is close to the results proposed by Hsiung [8]. These results proposed by Hsiung and this previous match quite well with measured results of wall deformation. This indicates that the proposed soil modulus $E_{50} = 2500N$ with As1, As2 layers; $E_{50} = 300S_u$ with Ac2 layer; $E_{50} = 500S_u$ with DC layer is suitable to compute the wall deformation of excavation. In contrast, from the figure, it can be observed that the application of E_{50} = PMT generally results in a greater wall deformation than measured values and other predicted methods. This result of PMT is not consistent with the result obtained in the previous study conducted by Hsiung [8], which may be explained by the small value of E from PMT as shown in Table 2.

4.2. Comparison between measured and predicted results for 3D models

The 3D influences on the wall deformation were computed using PSR, which is known as the ratio of the maximum deformation to its maximum wall deformation under plane strain conditions [2]. The results of wall deformation of 08 monitoring points using 3D models are presented in Fig. 9. Similar to the 2D models when the depth is larger than 20 m, the wall deformation results of measured values are smaller than those of predicted methods.

In addition, the wall deformation results from the PMT method are always far larger than those both of measured and other predicted methods. This is in agreement with the results obtained in 2D models. These results may be explained by the smaller soil modulus obtained from PMT tests, as shown in Table 2. From Fig. 9, it can be observed that the wall deformation of the proposed soil modulus $E_{50} = 2500N$ with As1, As2 layers; $E_{50}300S_u$ with Ac2 layer; $E_{50} = 500S_u$ with DC layer fits well with the results obtained from Hisung and Japan (JP)

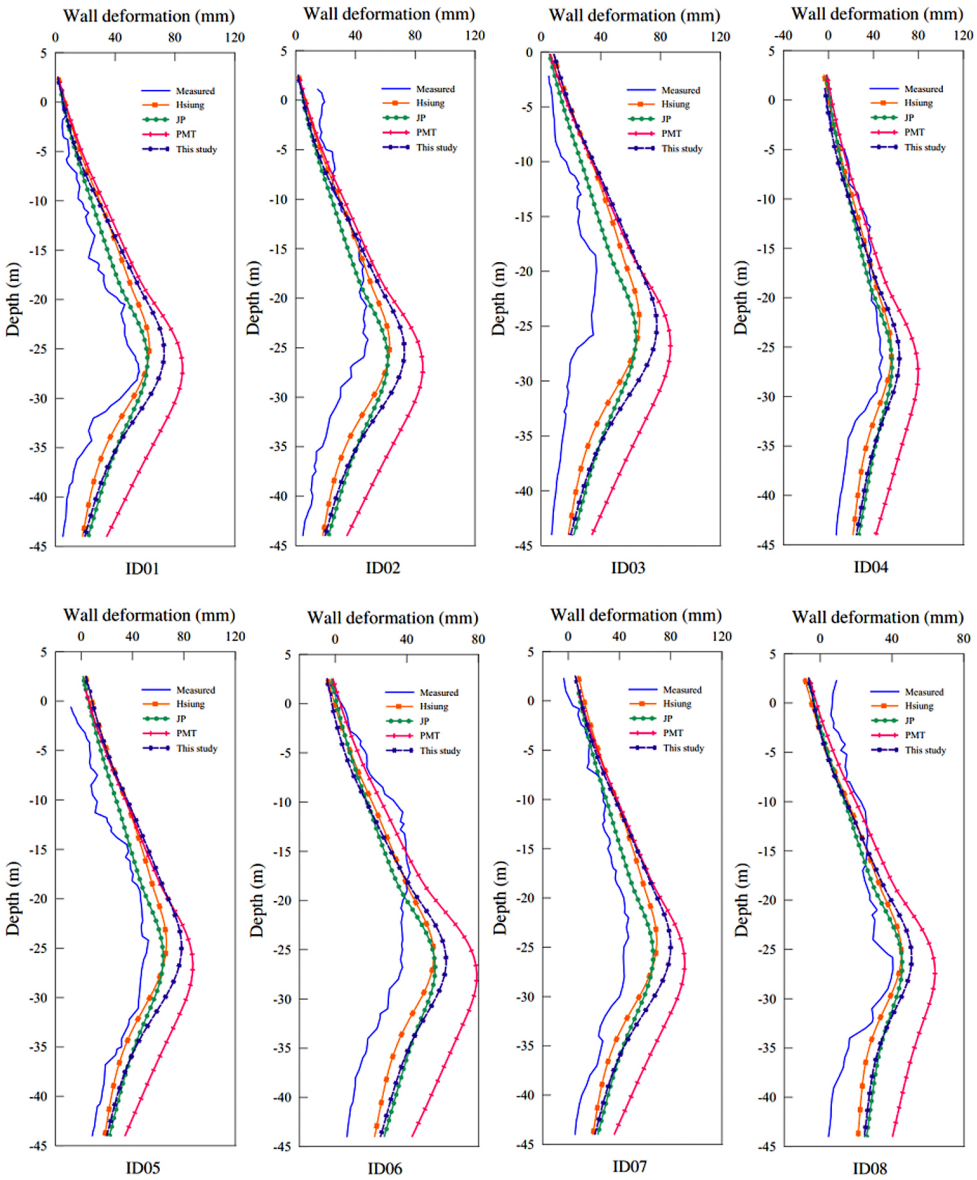

Fig. 8. Comparison of predicted and measured wall for the 2D model for 08 monitoring points

methods [8, 10]. Furthermore, the results of wall deformation in 3D models achieve similar values in comparison with the results obtained from 2D models. Thus, it can be inferred that the proposed soil modulus $E_{50} = 2500N$, $E_{50} = 300 \div 500S_u$ can be used to model the wall deformation of excavation for sand and clay layer.

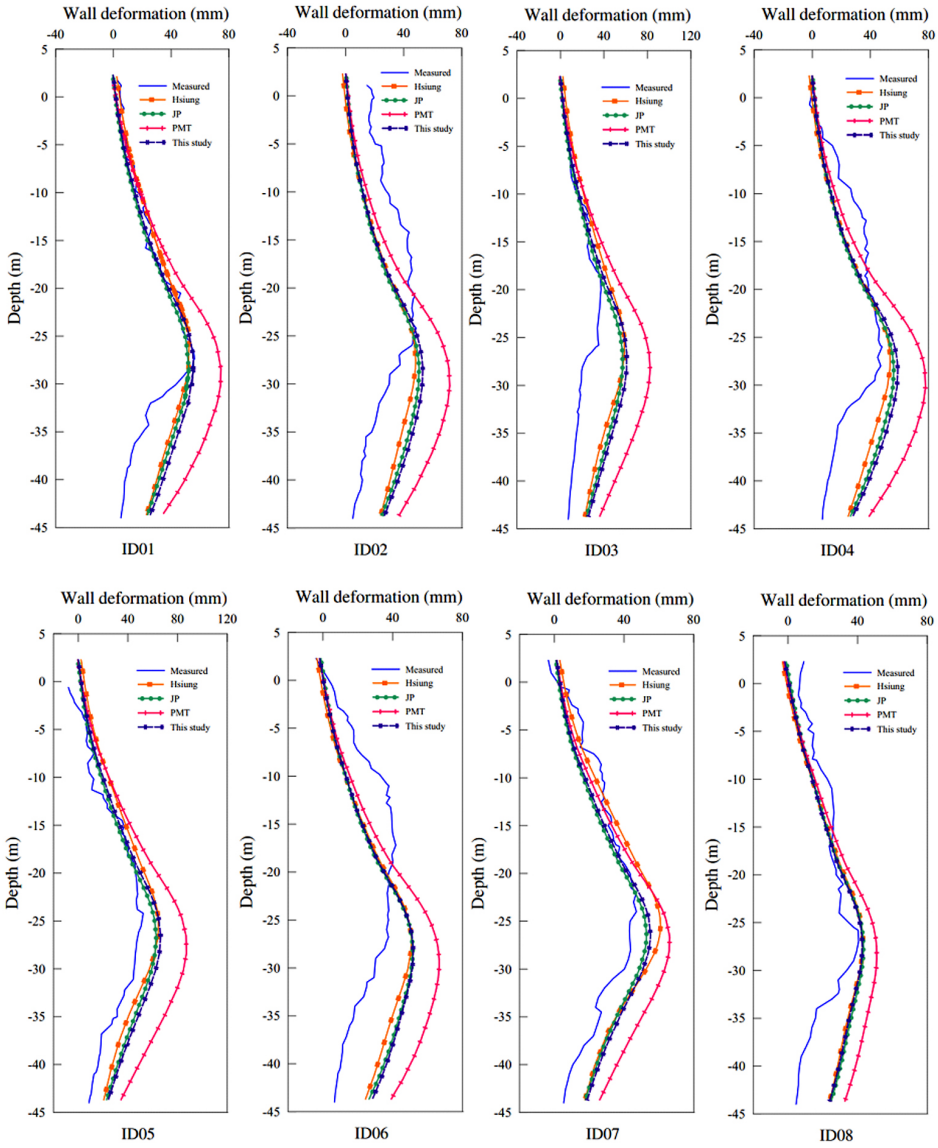

Fig. 9. Comparison of predicted and measured wall for the 3D model for 08 monitoring points

5. Conlusions

This study was conducted to evaluate the application of a hardening soil model to predict the wall deformation of excavation in 2D and 3D models at the Ho Chi Minh metro project, in Vietnam. In the 2D and 3D models, the soil stiffness modulus is verified on the basis of

the SPT test and PMT tet. A proposed method was used to compare with different predicted methods and measured results. Based on the results of the modeling, some conclusions can be drawn as follows:

- The soil stiffness modulus is a function of Nspt with sand layer, the soil stiffness modulus increases with depth.
- The results of wall deformation of 2D and 3D models were discussed and it was found that they have a good agreement.
- The proposed soil stiffness modulus $E_{50} = 2500N$, $E_{50} = 300 \div 500S_u$ can be used to model for sand, and clay layer is used for modeling wall deformation. The results of the proposed method match well with both measured results and predicted results from the previous studies. It indicates that the newly proposed method can be used for predicting the displacement of retaining for excavation in other projects.

References

[1] M.A. Nikolinakou, A.J. Whittle, S. Savidis, and U. Schran, "Prediction and interpretation of the performance of a deep excavation in Berlin sand", *Journal of Geotechnical and Geoenvironmental Engineering*, vol. 137, no. 11, pp. 1047–1061, 2011, doi: 10.1061/(ASCE)GT.1943-5606.0000518.

[2] C.-Y. Ou, D.-C. Chiou, and T.-S. Wu, "Three-dimensional finiteelement analysis of deep excavations", *Journal of Geotechnical Engineering*, vol. 122, no. 5, pp. 337–345, 1996, doi: 10.1061/(ASCE)0733-9410(1996)122:5(337).

[3] B.-C.B. Hsiung, "A case study on the behaviour of a deep excavation in sand", *Computers and Geotechnics*, vol. 36, no. 4, pp. 665–675, 2009, doi: 10.1016/j.compgeo.2008.10.003.

[4] B.-C.B. Hsiung, K.-H. Yang, W. Aila, and C. Hung, "Three-dimensional effects of a deep excavation on wall deflections in loose to medium dense sands", *Computers and Geotechnics*, vol. 80, pp. 138–151, 2016, doi: 10.1016/j.compgeo.2016.07.001.

[5] W. Powrie, R.J. Chandler, D.R. Carder, and G.V.R. Watson, "Back-analysis of an embedded retaining wall with a stabilizing base slab", *Proceedings of the Institution of Civil Engineers-Geotechnical Engineering*, vol. 137, no. 2, pp. 75–86, 1999, doi: 10.1680/gt.1999.370202.

[6] R.J. Jardine, D.M. Potts, A.B. Fourie, and J.B. Burland, "Studies of the influence of non-linear stress–strain characteristics in soil–structure interaction", *Geotechnique*, vol. 36, no. 3, pp. 377–396, 1986, doi: 10.1680/geot.1986.36.3.377.

[7] M. A. Stroud, "The standard penetration test – its application and interpretation", presented at Conference on Penetration Testing in the UK, Londres, 1989.

[8] B.-C.B. Hsiung, K.-H. Yang, W. Aila, and L. Ge, "Evaluation of the wall deflections of a deep excavation in Central Jakarta", *Tunnelling and Underground Space Technology*, vol. 72, pp. 84–96, 2018, doi: 10.1016/j.tust.2017.11.013.

[9] K.Y. Yong, "Learning lessons from the construction of Singapore Downtown line (DTL)", in *Proceedings of International Conference and Exhibition on Tunneling and Underground Space 2015*.

[10] S. Morino and K. Tsuda, "Design and construction of concrete-filled steel tube column system in Japan", *Earthquake Engineering and Engineering Seismology*, vol. 4, no. 1, pp. 51–73, 2003.

[11] M. Khoiri and C.-Y. Ou, "Evaluation of deformation parameter for deep excavation in sand through case histories", *Computers and Geotechnics*, vol. 47, pp. 57–67, 2013, doi: 10.1016/j.compgeo.2012.06.009.

[12] G.T. Kung, C.H. Juang, E.C. Hsiao, and Y.M. Hashash, "Simplified model for wall deflection and ground-surface settlement caused by braced excavation in clays", *Journal of Geotechnical and Geoenvironmental Engineering*, vol. 133, no. 6, pp. 731–747, 2007, doi: 10.1061/(ASCE)1090-0241(2007)133:6(731).

[13] H. Schweiger, "Design of Deep Excavations with FEM-Influence of Constitutive Model and Comparison of EC7 Design Approaches", in *Earth Retention Conference 3*. ASCE, 2010, doi: 10.1061/41128(384)81.

[14] H. Michalak and P. Przybysz, "Subsoil movements forecasting using 3D numerical modeling", *Archives of Civil Engineering*, vol. 67, no. 1, pp. 367–385, 2021, doi: 10.24425/ace.2021.136478.

[15] ACI CODE-318-19(22): Building Code Requirements for Structural Concrete and Commentary (Reapproved 2022), doi: 10.14359/51716937.

[16] J.M. Duncan and A.L. Buchignani, *An engineering manual for settlement studies*. Berkeley: Department of Civil Engineering, University of California, 1976.

Received: 2023-06-23, Revised: 2023-09-12